

## Atomic force microscopy investigation of polysilicon films before and after SIMS analysis: the effects of sample rotation

This article has been downloaded from IOPscience. Please scroll down to see the full text article.

1998 J. Phys.: Condens. Matter 10 1699

(<http://iopscience.iop.org/0953-8984/10/8/006>)

View [the table of contents for this issue](#), or go to the [journal homepage](#) for more

Download details:

IP Address: 171.66.16.209

The article was downloaded on 14/05/2010 at 12:19

Please note that [terms and conditions apply](#).

## Atomic force microscopy investigation of polysilicon films before and after SIMS analysis: the effects of sample rotation

S J Guilfoyle†§, A Chew†||, N E Moiseiwitsch‡, D E Sykes†|| and M Petty†||

† Department of Physics, Loughborough University, Loughborough LE11 3TU, UK

‡ 2029 Mountbatten Building, Department of Electronics and Computer Science, University of Southampton, Southampton SO17 1BJ, UK

Received 19 June 1997, in final form 18 December 1997

**Abstract.** Differences have been found in the depth resolution of dynamic SIMS profiles from polysilicon films on silicon carried out with and without sample rotation. Corresponding differences in the surface topography have been observed using atomic force microscopy. Both amorphous and polycrystalline silicon films implanted with fluorine and arsenic and subjected to rapid thermal annealing were examined. For the polycrystalline film, conventional SIMS analysis led to a significantly roughened crater, with a somewhat lesser roughening effect in the case of the rotational SIMS. The crater in the amorphous film showed slight roughening in the conventional analysis mode whereas with rotation the crater base appears to preserve the initial topography of the film.

### 1. Introduction

Secondary-ion mass spectrometry (SIMS) is widely used for the determination of the depth distribution of dopant and impurity species in semiconductor matrices. There are a number of artefacts that occur in the SIMS process that can distort the measured depth distribution, for example profile broadening due to atomic mixing, segregation effects arising from the incorporation of primary ion species in the matrix material, sputter-induced topography and transient effects in the region of the surface. These artefacts and their impact on ultra-shallow depth profiling have been thoroughly reviewed by Zalm [1] and others. In this work we are concerned with the effects of sputter-induced topography and their suppression.

The different artefacts influence the depth resolution to differing degrees, for example transient effects and atomic mixing are of more significance in the analysis of ultra-low-energy ion implantation or the shallow, thin epitaxial layers. Profile broadening due to surface topography is generally thought of as an effect which is only significant at depth, for example once the well known ripple formation, that occurs on silicon under oxygen ion bombardment, has developed [2]. The analysis of thin structures of polysilicon on silicon (for example polysilicon emitter structures) would not normally be thought to exhibit profile broadening due to ion-induced topography. However, in this study we

§ Present address: V G Elemental, Ion Path, Road Three, Winsford, Cheshire CW7 3BX, UK.

|| Present address: Loughborough Surface Analysis Ltd, PO Box 5016 Unit RFC, Gas Research Centre, Ashby Road, Loughborough, Leicestershire LE11 3WS, UK.

demonstrate that topographical broadening can occur in 300 nm thick polysilicon layers and that sample rotation, which has been used successfully by ourselves and others to overcome topographical broadening in other material systems [3–5], can be used in this case to overcome the broadening.

## 2. Experiment

Two samples consisting of either amorphous or polycrystalline silicon films deposited onto p-type (100) 4 in silicon wafers were fabricated in the following way. The wafers were given an initial RCA surface treatment and then loaded immediately into an LPCVD polysilicon reactor. Following this, a nominal 400 nm of Si was deposited at either 560 °C (for amorphous Si) or 610 °C (for polycrystalline Si). Next a fluorine (F<sup>+</sup>) implant of  $1 \times 10^{16} \text{ cm}^{-2}$  at 50 keV was performed, followed by an arsenic (As<sup>+</sup>) implant of  $1 \times 10^{16} \text{ cm}^{-2}$  at 70 keV. A 600 nm blanket layer of low-temperature LPCVD oxide (SiO<sub>2</sub>) was deposited as a capping layer to prevent the out-diffusion of the arsenic from the polysilicon layer. The wafers were then broken into 15 mm squares and annealed in a rapid thermal processor on top of a silicon susceptor. The annealing temperature was fixed at 1015 °C with samples being annealed for 90 seconds. This was done to promote phase separation of the dopant material and to investigate the effect of heat treatment on the epitaxy of the substrate/film interface. Before analysis the low-temperature oxide layer was removed by wet etching.

The SIMS analysis was carried out in a Cameca IMS-3F detecting positive secondary ions and using O<sub>2</sub><sup>+</sup> bombardment with a 10 kV source potential giving an impact energy of 5.5 keV (2.75 keV per oxygen atom) at an angle of incidence of 42° to the sample normal. The primary ion beam was rastered over an area nominally 250 μm square, with secondary ions collected from a central 60 μm diameter area. Sample rotation was carried out using a Kore rotation stage which has been described elsewhere [6]; a rotation speed of approximately 3 rpm was used.

Surface topography measurements were made using a Burleigh ARIS 3300 Personal AFM. Measurements were performed in air. The piezo scanner had a maximum lateral scan range of 5 μm. The maximum resolution normal to the sample surface was of the order of 0.1 nm. A 442 μm long cantilever (Burleigh Standard AFM probe) with an integrated silicon tip was used. The silicon tips were 10–15 μm long, with an aspect ratio of 1:1 and an end radius of 10 nm. The images were acquired using a total scan time of about 200 seconds. The tilt of the sample was corrected in the software using a slope correction applied to the whole image. A line removal was also performed to remove scanning artefacts.

## 3. Results and discussion

Figure 1(a) and (b) shows SIMS data for the polysilicon film sputtered to a total depth of 500 nm. Trace (a) corresponds to the normal SIMS profile. In this profile the fluorine peaks occur at depths of 0.32 μm, in the substrate/film interface, and a depth of 0.11 μm, at approximately the mean projected range of the implanted fluorine. These features are fairly broad, corresponding to FWHM values of 0.08 and 0.18 μm respectively. These maxima in the fluorine concentration are due to the residual implant peak and fluorine which has diffused to the polysilicon/silicon interface. The depth profile for the same sample rotated at 3 rpm is shown in figure 1(b). Here the substrate/film interface fluorine peak for the rotational sample is much sharper, again occurring at 0.32 μm and corresponding to a

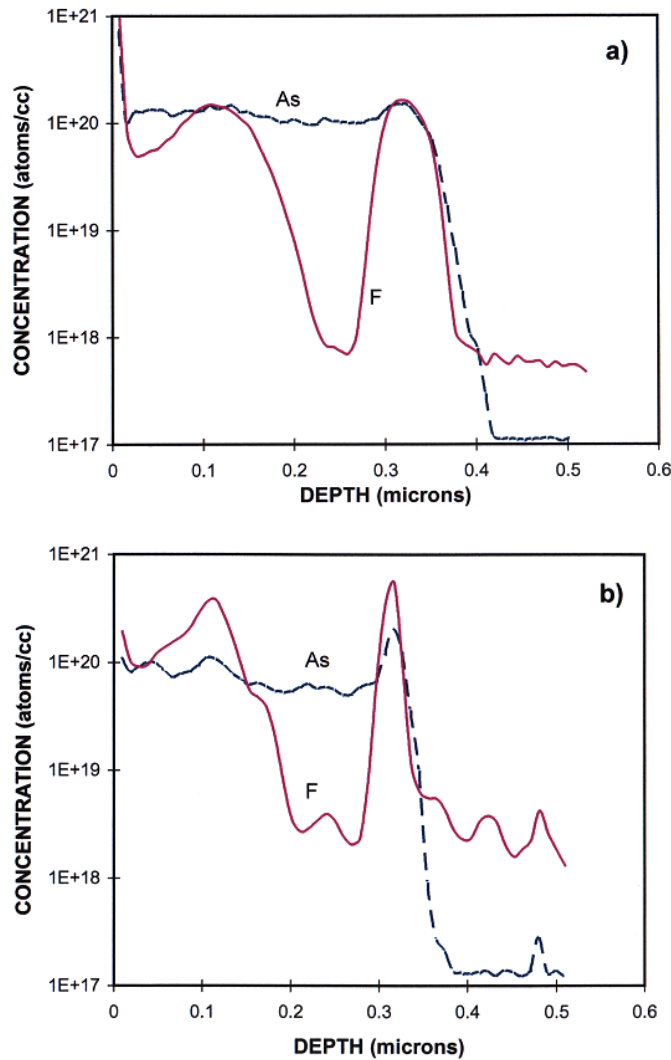


**Figure 1.** SIMS data for a polysilicon film sputtered to a depth of 500 nm. Trace (a) corresponds to the dynamic SIMS profile and (b) to the profile with the sample rotating at 3 rpm.

FWHM of  $0.04 \mu\text{m}$ . The apparently Gaussian implant feature seen in figure 1(a) now contains additional structure. This increase in the information content of the profile is indicative of an increase in depth resolution due to the suppression of the surface topography.

The SIMS results for the amorphous silicon film are shown in figure 2. In this case there is less difference between the non-rotated and rotational results, with both sets of data approximating that of the rotational SIMS for the polycrystalline sample shown in figure 1(b). Work by Szeles *et al* [7] suggests that the fine structure seen in these profiles, i.e. the shoulders around the fluorine peak with the polysilicon layers, may result from the immobilization of the fluorine at damage sites produced after the arsenic and fluorine ion implantation into the polysilicon layer.

AFM scans were acquired of the polycrystalline and the amorphous samples in the as-

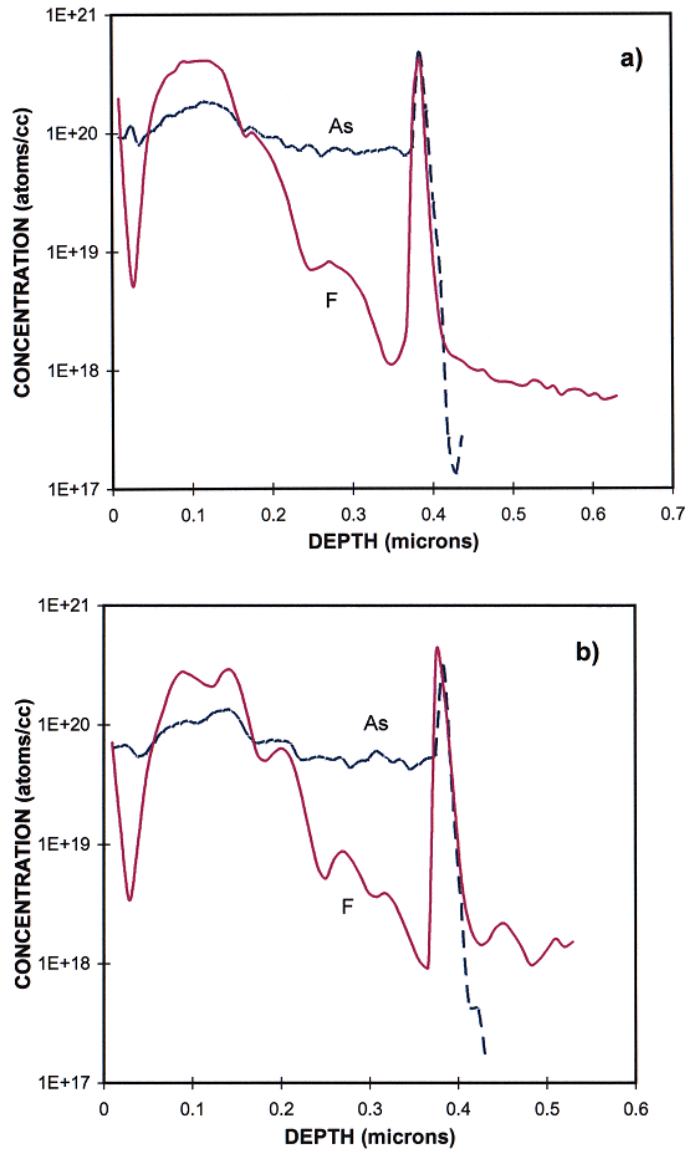
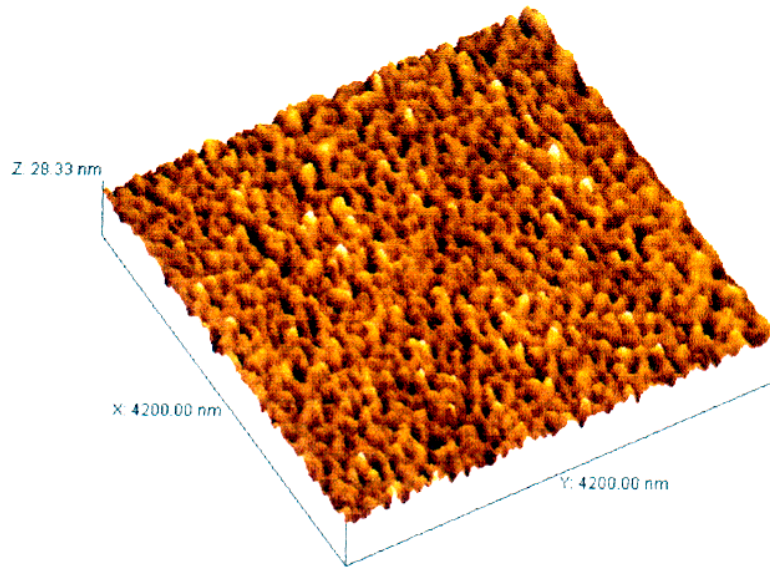


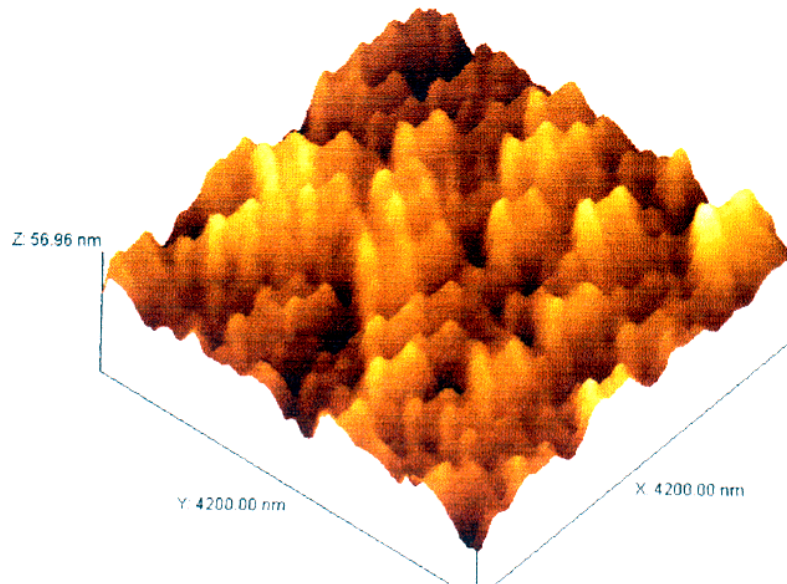
**Figure 2.** SIMS data for an amorphous silicon film sputtered to a depth of 500 nm. The first trace (a) corresponds to the dynamic SIMS profile and (b) to the profile with the sample rotating at 3 rpm.

annealed state before SIMS analysis and from the SIMS craters of both samples. All of the scans were recorded as  $256 \times 256$  pixel images over identical (4 mm) scan areas.

By using the software supplied by Burleigh, RMS values of the roughness around the mean surface level were obtained ( $H_{RMS}$ ). These calculations were performed over the entire area of each AFM scan. The values can be used as a comparison of the surface roughness of different samples. The AFM scans are displayed as three-dimensional plots to give an easily comparable impression of depth.



(a)



(b)

**Figure 3.** AFM images of the polycrystalline silicon film before SIMS analysis (a), and following dynamic (b) and rotational (c) SIMS analysis.

Figure 3 shows a comparison of the polycrystalline Si film before SIMS analysis (a) and images of the dynamic SIMS crater (b) and rotational SIMS crater (c). In figure 3(a) a series of regular features with in-plane dimensions of about 100 nm and a vertical height of 10–15 nm can be seen. The  $H_{RMS}$  value for this surface is 4.73 nm. These features are somewhat large for a film deposited in this way. Examination of the non-rotated SIMS

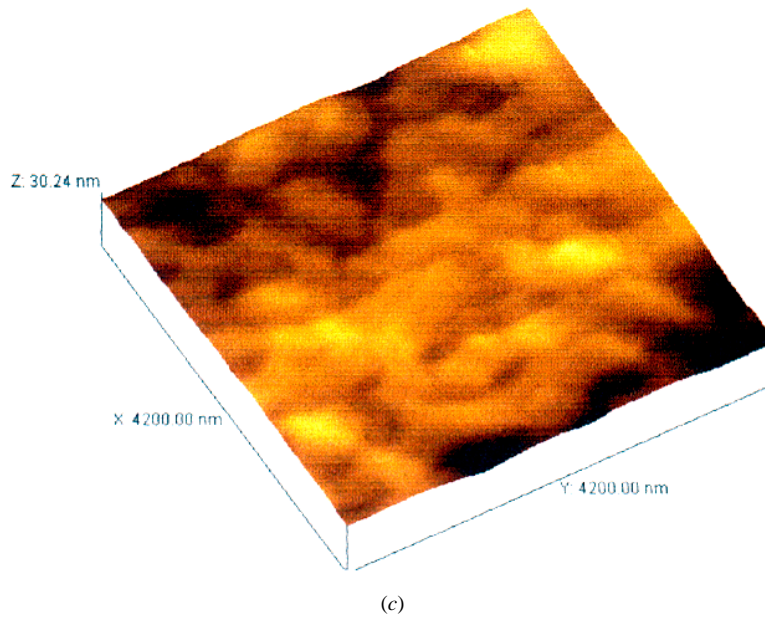


Figure 3. Continued.

crater reveals more irregular features of significantly increased size both in plane (200–300 nm) and along the vertical direction (20–50 nm) leading to an  $H_{RMS}$  value of 9.49 nm. In comparison to this, the rotational SIMS produces features which have larger in-plane dimensions but are much flatter. That is, whilst the vertical height of the features is similar to that of the as-annealed surface, the  $x$  and  $y$  plane dimensions are of the order of 600 nm. The  $H_{RMS}$  value is 5.05 nm, which is close to that of the unspattered surface. Repeating these measurements several times produces values within 5% of the results quoted.

Figure 4 shows the amorphous film before SIMS analysis (a) and following dynamic (b) and rotational SIMS analysis (c). The initial surface is somewhat smoother than that of the polycrystalline sample, with an  $H_{RMS}$  value of 0.41 nm. SIMS profiling of the amorphous film produces the characteristic ripple topography with wavelengths of 300–400 nm and a vertical height  $H_{RMS}$  of 3–6 nm. However, the rotational SIMS appears to produce a surface which is unchanged from the initial state, with features less than a nanometre in height. The unanalysed surface and the non-rotated SIMS crater lead to  $H_{RMS}$  values of 0.41 nm and 1.50 nm respectively. In comparison to this, the rotational SIMS  $H_{RMS}$  is found to be 0.44 nm.

Considering first the polycrystalline sample, it appears that the SIMS leads to a considerably roughened surface and a subsequent loss of the depth resolution. The preferential etching of crystallites with differing surface orientations by the ion beam leads to a smeared interface over which data collection occurs, broadening the fluorine film/substrate interface peak. The rotated sample shows less surface roughness (though the features are somewhat increased in lateral dimensions), which correlates with the sharper more abrupt fluorine peak.

For the case of the amorphous film, the initial surface is comparatively smooth, and the rotational SIMS appears to have no effect at all on the topography. Hence the rotational SIMS technique is a suitable method to preserve the initial topography of an amorphous

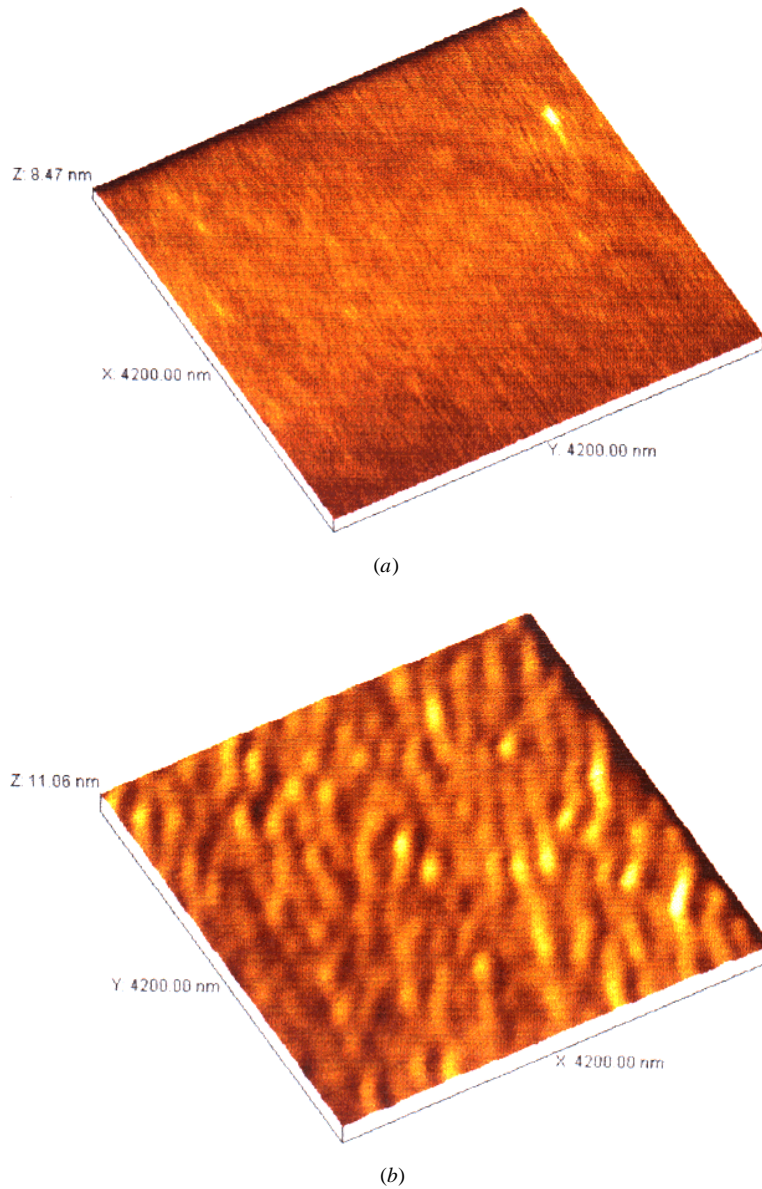


**Figure 4.** AFM images of the amorphous silicon film before SIMS analysis (a), and following dynamic (b) and rotational (c) SIMS analysis.

surface. The non-rotated SIMS has the effect of causing characteristic ripples, though these features are relatively small compared to those from the polycrystalline sample and so the effect on the SIMS data is minimal. The ripples may also be present in the polycrystalline sample but would be hidden by the more significant effect of the differential sputtering. Thus, for polycrystalline films in particular, AFM data are in agreement with previous SEM data [4] that target rotation is a suitable method for improving the SIMS resolution.



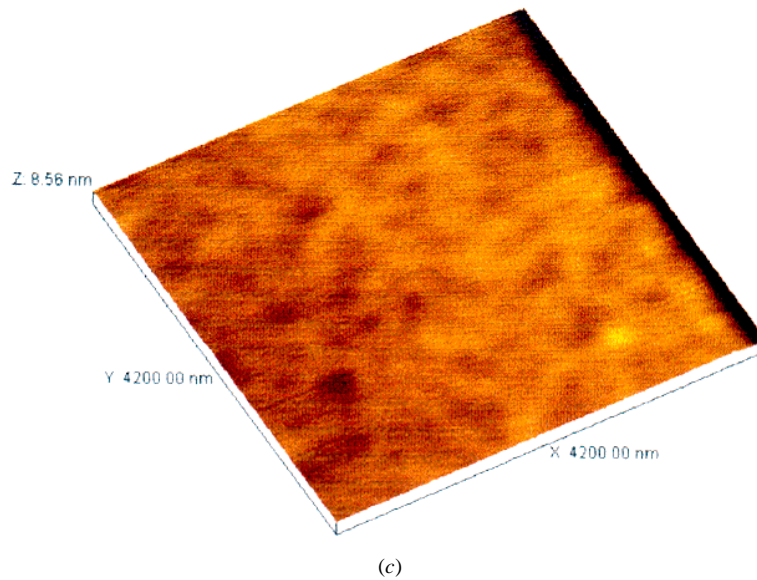


Figure 4. Continued.

#### 4. Conclusion

Samples consisting of either amorphous or polycrystalline doped silicon were deposited onto silicon substrates and annealed. SIMS analysis was performed on the samples using both the traditional non-rotated technique and also using a sample rotation technique. It was found that for the polycrystalline sample, in particular, the non-rotated SIMS led to fluorine peaks of increased width, indicating reduced resolution. Topographical analysis using AFM revealed that the craters in the polycrystalline surface were significantly rougher than when the rotational technique was applied. For the case of the amorphous sample the discrepancy between the non-rotated SIMS and rotational SIMS data was somewhat less. In addition, the rotational analysis appeared to preserve the topography of the initial unsputtered surface. Therefore, for the most accurate SIMS data the rotational analysis of an amorphous surface is required.

#### Acknowledgments

The support of the LINK Enhanced Magnetic Materials Initiative (grant number 12/5/56) is gratefully acknowledged.

#### References

- [1] Zalm P 1994 *Rep. Prog. Phys.* **58** 1321
- [2] Stevie F A, Kahora P M, Simons D S and Chi P 1988 *J. Vac. Sci. Technol. A* **6** 76
- [3] Sykes D E and Chew A 1994 *Surf. Interface Anal.* **21** 231
- [4] Cirlin E-H and Vajo J J 1992 *SIMS VIII* (Chichester: Wiley) p 347
- [5] Stevie F A and Moore J L 1992 *Surf. Interface Anal.* **18** 147
- [6] Chew A, Sykes D E, Mullock S J and Corlett C A 1994 *SIMS IX* (Chichester: Wiley) p 302
- [7] Szeles Cs, Nielsen B, Asoka-Kumar P, Lynn K G, Anderle M, Ma T P and Rubloff G W 1994 *J. Appl. Phys.* **76** 3403